TECHNICAL REPORT ARBRL-TR-02530

THERMAL-ENERGY TRANSPORT FROM ARC TO RAILS IN AN ARC-DRIVEN RAIL GUN

John D. Powell

October 1983

US ARMY ARMAMENT RESEARCH AND DEVELOPMENT CENTER
BALLISTIC RESEARCH LABORATORY
ABERDEEN PROVING GROUND, MARYLAND

Destroy this report when it is no longer needed.
Do not return it to the originator.

Additional copies of this report may be obtained from the National Technical Information Service, U. S. Department of Commerce, Springfield, Virginia 22161.

The findings in this report are not to be construed as an official Department of the Army position, unless so designated by other authorized documents.

The use of trade names or manufacturers' names in this report does not constitute indorsement of any commercial product.

REPORT DOCUMENTATION PAGE

READ INSTRUCTIONS BEFORE COMPLETING FORM

1. REPORT NUMBER: TECHNICAL REPORT ARBRL-TR-02530
2. GOVT ACCESSION NO.:
3. RECIPIENT'S CATALOG NUMBER:

4. TITLE (and Subtitle): THERMAL-ENERGY TRANSPORT FROM ARC TO RAILS IN AN ARC-DRIVEN RAIL GUN

5. TYPE OF REPORT & PERIOD COVERED:

6. PERFORMING ORG. REPORT NUMBER:

7. AUTHOR(s): John D. Powell

8. CONTRACT OR GRANT NUMBER(s):

9. PERFORMING ORGANIZATION NAME AND ADDRESS:
US Army Ballistic Research Laboratory, ARDC
ATTN: DRSMC-BLB
Aberdeen Proving Ground, MD 21005

10. PROGRAM ELEMENT, PROJECT, TASK AREA & WORK UNIT NUMBERS:
RDT&E 1L162603AH18

11. CONTROLLING OFFICE NAME AND ADDRESS:
US Army AMCCOM, ARDC
Ballistic Research Laboratory, ATTN: DRSMC-BLA-S(A)
Aberdeen Proving Ground, MD 21005

12. REPORT DATE: October 1983

13. NUMBER OF PAGES: 37

14. MONITORING AGENCY NAME & ADDRESS (if different from Controlling Office):

15. SECURITY CLASS. (of this report): Unclassified

15a. DECLASSIFICATION/DOWNGRADING SCHEDULE:

16. DISTRIBUTION STATEMENT (of this Report)
Approved for public release; distribution unlimited.

17. DISTRIBUTION STATEMENT (of the abstract entered in Block 20, if different from Report)

18. SUPPLEMENTARY NOTES

19. KEY WORDS (Continue on reverse side if necessary and identify by block number)

Electric gun	Rail gun
Electromagnetic propulsion	Arc dynamics
Thermal-energy transfer	Rail melting

Heat transfer
Thermodynamics
Energy transport

20. ABSTRACT (Continue on reverse side if necessary and identify by block number) (idk)

A model is developed for examining thermal-energy transfer from the arc to the rails in an arc-driven rail gun. Resistive heating within the rails is also accounted for, though the contribution to the rail temperature from this mechanism is frequently negligible. Melting of the rail surface is allowed in the model, but it is assumed that the melted material is swept away and absorbs no further energy. A set of differential equations is derived which, when solved, yield the temperature, magnetic induction, and current density (continued)

within the rail, as well as the mass lost from the rail surface. Both numerical and limiting-case analytic solutions to the equations are presented, and approximate expressions are obtained for the "time to melting" and the steady-state "melting velocity" of the rail surface. It is found that the governing equations can be written in a form so that they depend only on experimentally measured properties of the arc. The model is then used to analyze rail melting in a recent experiment by Jamison and Burden, for which these properties have been obtained. It is also used to estimate rail damage in other experiments by using arc properties calculated in our previous work. Considerable discussion is given of the probable sources of error in the calculation and recommendations for improvements in future work are made.

TABLE OF CONTENTS

LIST OF FIGURES

I. INTRODUCTION

In recent work, one-[1] and two-dimensional[2] calculations of the properties of arcs in arc-driven rail guns were carried out. The principal purpose of that work was two-fold. First, we wanted to determine the most reasonable arc materials and whether, by a judicious choice of material, we could control the arc's thermodynamic properties. Second, we wanted to provide the basis for investigating what erosive effects the arc had on the rails and projectile. In the present work we undertake a preliminary investigation of what the erosive effects are.

Specifically, we wish to provide a simple model for determining thermal-energy generation in and transfer to the rails, and for assessing the damage to the rails caused by that thermal energy. The energy generated in the rails will be assumed to arise from ohmic heating, while that transferred from the arc to the rails will be assumed to be radiative. Although extensive experimental work designed to examine carefully rail damage has not been carried out, early work has indicated the greatest damage near the breech end of the gun, but practically none farther down the gun tube. It is not clear, however, that even at the breech end, the damage is thermal in origin and it is important to determine theoretically under what conditions such damage might be significant.

The model used in Refs. 1 and 2 is shown schematically in Fig. 1. Initially, the rails (the upper and lower sides in the figure), which are infinitely extended in the z direction, are supplied a pulsed current i_0 which is assumed to be constant in time and which flows in the direction indicated. In our previous work the rails were assumed to be perfect conductors so that the current was carried only along their inner surface and their thickness was insignificant; in the figure, however, we have indicated the finite thickness d of the rails. For finite conductivity, of course, the current is carried within some skin depth Δ from the rail surface. The current is also conducted through the arc which has length ℓ_a. The resulting current configuration then produces a magnetic field between the rails in the space bounded by the power supply and the arc, as well as in the arc itself. This induction field, in turn, interacts with the current through the arc producing a high-pressure plasma which accelerates the projectile, shown by the shaded area, in the x direction. One- and two-dimensional calculations were undertaken to determine the properties of the arc under the assumption that those properties were steady as seen by an observer in the accelerating reference frame. Some justification for the steady-state approximation was given for the acceleration times of interest.

In the present calculation we wish to consider the problem of thermal-energy transfer from the arc to the rails. For completeness, we will also account for resistive heating in the rails, though in most practical problems

[1] *J.D. Powell and J.H. Batteh, "Plasma Dynamics of an Arc-Driven, Electromagnetic, Projectile Accelerator," J. Appl. Phys. 52, 2717 (1981). See also "Plasma Dynamics of an Arc-Driven Rail Gun," Ballistic Research Laboratory Report No. ARBRL-TR-02267, September 1980 (AD A092345).*

[2] *J.D. Powell and J.H. Batteh, "Two-Dimensional Plasma Model for the Arc-Driven Rail Gun," J. Appl. Phys. 54, 2242 (1983). See also J.D. Powell, "Two-Dimensional Model for Arc Dynamics in the Rail Gun," Ballistic Research Laboratory Report No. ARBRL-TR-02423, October 1982 (AD A120046).*

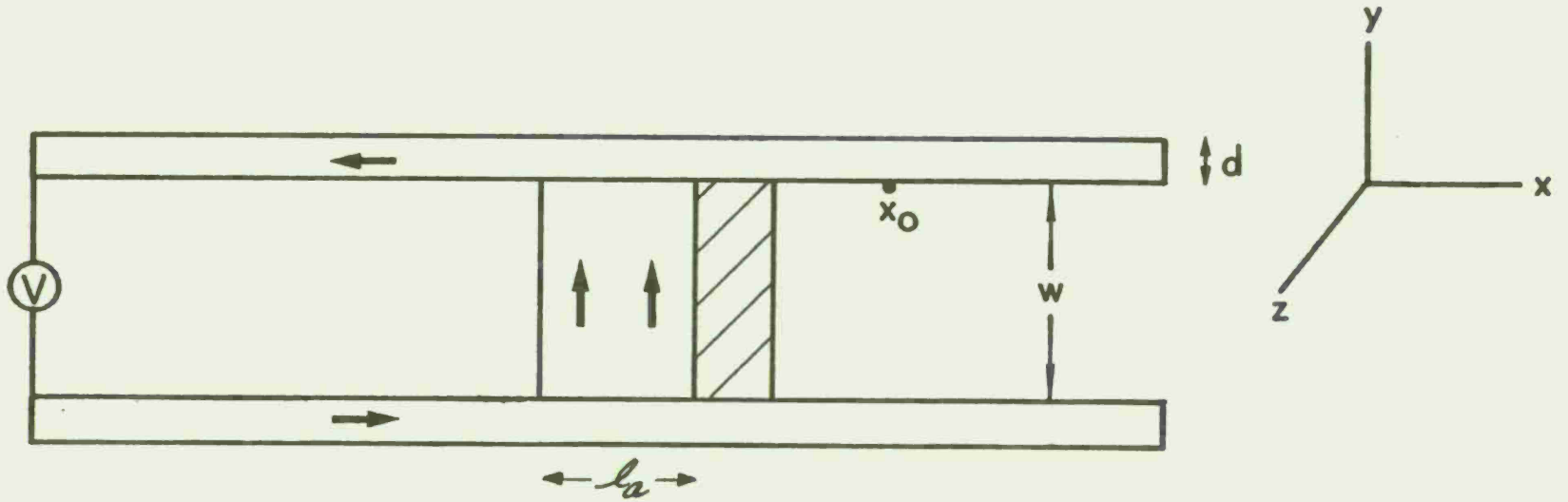

Figure 1. Rail gun model.

resistive heating is insignificant compared to heating from the arc, especially if the rail thickness is comparable to or larger than the electrical skin depth.

Consider the point x_0 in Fig. 1. When the leading edge of the arc reaches the point, the temperature there will rise both because of heat transfer from arc to rail, as well as because of ohmic heating initiated in the rail once current begins to flow. Once the arc has completely passed x_0, radiative transfer from arc to rail is assumed to be small, though the temperature in the interior of the rail still rises because of ohmic heating. If and when the temperature at the rail surface reaches the melting temperature, T_m, the temperature there will remain constant but the surface will recede from its initial position at $y = 0$. Therefore, the location of the rail surface is a time-dependent quantity given by $y = s(t)$, and the magnitude of $s(t)$ is indicative of the mass lost at the gun-tube surface due to melting. We want to calculate the location of the surface as well as the temperature, magnetic induction, and current density within the rail.

The calculation is characterized by a number of assumptions made to make the analysis as simple as possible. Perhaps the most significant is that the arc-dynamic problem can be uncoupled from the rail-heating problem. It is, for example, assumed that the radiation flux from the arc incident on the surface of the rails is independent of time and unaffected by the rise in the rail temperature. As has been argued before,[1] such an assumption is clearly reasonable since the arc temperature is more than an order of magnitude higher than that of the rails. The arc serves, therefore, essentially as a high-temperature reservoir whose thermodynamic properties are nearly steady, while those of the rails are quite unsteady. It is also assumed that the magnetic flux density at the rail-arc interface varies linearly from zero at the front of the arc to μj at the back of the arc. Here μ is the magnetic permeability and j is given by

$$j = \int_0^d J_x(x_0,y)\, dy, \tag{1.1}$$

where $\vec{J}$ is the current density in the rails and d is the rail thickness. That the induction field should take on these values in front of and behind the arc can be proved easily by Ampere's law. While the linear variation at the interface is not strictly correct for the problem at hand, it would be valid if the rails were perfect conductors and if the conductivity of the arc were constant, and it is nearly valid for more realistic values of the arc conductivity.[1,2] For rails which are not perfect conductors, determining the value of the induction field at the interface would necessitate solving the magnetic diffusion equation in both the rails and arc, and applying the appropriate boundary conditions at the interface. For such a calculation the electromagnetic properties of the arc are coupled to those of the rails. We expect, however, that since the rail conductivity is several orders of magnitude higher than that of the arc, the assumption of perfect conductivity is satisfactory for determining the interface boundary condition. Furthermore, any errors made in such an assumption should be insignificant since, in practical problems, while the arc is in contact with the point x_0, the dominant mechanism for heat production there is radiation from the arc.

The second principal assumption is that all the radiative flux from the arc that is incident on x_0 is absorbed by the rails, just as if the arc were radiating into a vacuum. No doubt some of this incident energy is reflected back into the arc, but it is difficult to estimate how much. Furthermore, by assuming total absorption, we should overestimate the erosive effects on the rails and can easily alter the heat flux when more reliable estimates are known. The value of the heat flux incident on the rails is assumed to be given by

$$Q = 2 \sigma_s T_b^4 \tag{1.2}$$

where T_b is the arc temperature at the boundary and where σ_s is Stefan's constant, namely, $5.67 \times 10^{-8} \frac{J}{m^2 K^4 s}$. This approximate expression has been discussed elsewhere.[1,2]

The third major assumption is that any melted portion of the rails is "swept away" by the motion of the arc so that the radiation flux is always incident on the solid rail surface. It might appear that such an assumption would be unreasonable because one would expect that the liquid rail material would remain on the surface because of inertial effects during the time of interest (tens of microseconds). However, for the problem at hand, the pressures at the rail surface are of the order of hundreds of atmospheres and these large pressures may indeed produce large-scale motion during the time of contact. At any rate, the assumption should again overestimate the erosive effects since none of the energy is expended in heating the liquid or gaseous phase.

Three additional assumptions in the calculation merit brief mention. First, we will neglect diffusion within the rail of both the magnetic induction field and the temperature in the direction of propagation, and assume that it occurs only in the y direction. The assumption is likely to be valid for projectile velocities that are high compared to the speed with which both quantities can diffuse into the rail. Such is the case in any practical experiment. Second, we will assume that the major form of energy transport within the rails is ordinary heat conduction and will neglect radiation. That radiation is negligible below the melting temperature of rail materials is easily demonstrated. Finally, we neglect the temperature dependence of the electrical and thermal conductivities and of the specific heat of the rails. This assumption is made partly because reliable expressions are not known everywhere in the temperature range under consideration, and partly because analytic solutions can be obtained in special cases and these provide a useful comparison with the numerical solutions.

II. FORMALISM

Consider point x_0 in Fig. 1 and note that prior to acceleration the leading edge of the arc is located at $x = 0$. Then since the acceleration a is constant, the arc velocity when the leading edge reaches x_0 is given by

$$v_0 = (2a\, x_0)^{1/2} \quad . \tag{2.1}$$

If we denote this time by t = 0, we can write that in time t the leading edge will move beyond x_0 by a distance D given by

$$D = v_0 t + 1/2\, a\, t^2 \quad . \tag{2.2}$$

Furthermore, since it is assumed that the magnetic induction field varies linearly from zero to μj as one moves from the front to the rear of the arc, we clearly have at x_0

$$\begin{aligned} B(s,t) &= \frac{\mu j}{\ell_a}\,(v_0 t + 1/2\, a\, t^2) \qquad t \leq t_0 \\ B(s,t) &= \mu j \qquad\qquad\qquad\qquad t > t_0 \quad . \end{aligned} \tag{2.3}$$

Here ℓ_a represents the total length of the arc and t_0 is the time for which the arc is in contact with the point x_0. One can easily show that

$$t_0 = \sqrt{2/a}\,(\sqrt{x_0 + \ell_a} - \sqrt{x_0}\,) \quad . \tag{2.4}$$

Given the time-dependent boundary condition at y = s, the B field for y > s can be determined from the magnetic diffusion equation

$$\mu\sigma \frac{\partial B}{\partial t} = \frac{\partial^2 B}{\partial y^2} \quad , \tag{2.5}$$

where diffusion in x direction has been neglected to accord with the assumptions in Sec. I. The current density then follows from the relation

$$J = J_x = \frac{1}{\mu}\frac{\partial B}{\partial y} \quad . \tag{2.6}$$

Heat conduction in melting solids has been considered by various authors. Probably the treatment most closely related to the present work is that by Landau[3] to which the reader is referred for additional references. Generally we can write the energy-conservation relation within the rail as

$$\rho\, C \frac{\partial T}{\partial t} + \frac{\partial q}{\partial y} = J^2/\sigma - E_L \tag{2.7}$$

---

[3] *H.G. Landau, "Heat Conduction in a Melting Solid," Quart. Appl. Math. 8, 81 (1950).*

where ρ represents the solid-phase density, C is the specific heat, T the temperature, q the heat flux, σ the electrical conductivity, and E_L the energy absorbed per unit volume and time by the solid in the melting process. If we identify the term J^2/σ as the energy dissipated per unit volume and time arising from resistive heating, the physical meaning of Eq. (2.7) is apparent.

Now if the solid-liquid transition takes place at a well-defined temperature T_m as for most metals, we can write

$$E_L = L\rho\, \delta(T-T_m)\, \frac{\partial T}{\partial t} \tag{2.8}$$

where δ is a Dirac delta function and L is the heat of fusion, i.e., the heat absorbed per unit mass of solid to produce an equivalent amount of liquid. Furthermore, from properties of the delta function,

$$\delta(T-T_m) = \frac{1}{\left| \frac{\partial T}{\partial y} \right|_{y=s}}\, \delta(y - s) \ . \tag{2.9}$$

It is evident on physical grounds, however, that

$$\left(\frac{\partial T}{\partial y}\right)_{y=s} < 0 \tag{2.10}$$

and that at $y = s$, T changes only by virtue of the moving boundary. Consequently, it follows that

$$\left(\frac{\partial T}{\partial t}\right)_{y=s} = - \frac{ds}{dt} \left(\frac{\partial T}{\partial y}\right)_{y=s} , \tag{2.11}$$

and Eq. (2.7) finally becomes

$$\rho C \frac{\partial T}{\partial t} + \frac{\partial q}{\partial y} = \frac{J^2}{\sigma} - L\rho \frac{ds}{dt}\, \delta(y - s) \ . \tag{2.12}$$

The last term in Eq. (2.12) is zero except at $y = s$ and the boundary conditions to which it gives rise can be obtained by integrating Eq. (2.12) across a negligibly small interval centered at $y = s$. We find

$$q\,(s + \varepsilon) - q\,(s - \varepsilon) = - L\rho \frac{ds}{dt} \ . \tag{2.13}$$

At $s - \varepsilon$ the flux is just that incident from the arc, namely,

$$Q = 2 \sigma_s T_b^4 \quad ; \tag{2.14}$$

at $s + \epsilon$ we have, assuming that ordinary heat conduction is dominant,

$$q = - k \frac{\partial T}{\partial y} \tag{2.15}$$

where k is the rail thermal conductivity. Thus, Eq. (2.13) becomes

$$k \left(\frac{\partial T}{\partial y}\right)_{y=s} = L\rho \frac{ds}{dt} - Q \quad . \tag{2.16}$$

Equations (2.5), (2.6), (2.12) and (2.16) are now sufficient, with the boundary conditions discussed, to determine the temperature, magnetic induction, current density, and boundary location. It must be remembered, however, that melting will temporarily cease if $T(s,t)$ drops below T_m, and in that case, $\frac{ds}{dt}$ becomes zero. It is convenient to transform the governing equations to a frame of reference that moves with the melting boundary, so we let

$$\eta = y - s(t) \tag{2.17}$$

and obtain

$$\mu\sigma \frac{\partial B}{\partial t} = \frac{\partial^2 B}{\partial \eta^2} + \mu\sigma \frac{ds}{dt} \frac{\partial B}{\partial \eta} \tag{2.18}$$

$$J = \frac{1}{\mu} \frac{\partial B}{\partial \eta} \tag{2.19}$$

$$\rho C \frac{\partial T}{\partial t} = \frac{J^2}{\sigma} + \frac{\partial}{\partial \eta} \left(k \frac{\partial T}{\partial \eta}\right) + \rho C \frac{ds}{dt} \frac{\partial T}{\partial \eta} \tag{2.20}$$

$$Q = - k \left(\frac{\partial T}{\partial \eta}\right)_{\eta=0} + L\rho \frac{ds}{dt} \quad . \tag{2.21}$$

These equations must be solved subject to the boundary and initial conditions:

$$B(0,t) = \frac{\mu j}{\ell_a}(v_0 + 1/2\ a\ t^2) \qquad t < t_0$$

$$B(0,t) = \mu j \qquad t > t_0$$

$$B(\eta,0) = 0 \qquad (2.22)$$

$$B(d-s,t) = 0$$

$$\left(\frac{\partial T}{\partial \eta}\right)_{\eta=d-s} = 0$$

$$T(\eta,0) = T_0$$

$$\frac{ds}{dt} > 0 \Rightarrow T(0,t) = T_m$$

where T_0 is the ambient temperature.

III. CALCULATIONS

A. Special-Case Analytic Solutions

We will be concerned primarily in this section with obtaining numerical solutions to Eqs. (2.18)-(2.21). Prior to undertaking the numerical calculations, however, it is useful to carry out some special-case analytic solutions for checking the computer program as well as giving some physical insight into the nature of the solution when special conditions apply. It will be assumed in this section that the rails are infinitely thick, an assumption that is reasonable provided the rail thickness d is large compared to the electrical skin depth. This condition is satisfied in all cases that will be considered.

Preparatory to carrying out the analytic solutions, it is useful to point out the following general results.[4] Consider the one-dimensional diffusion equation of the form

$$\frac{\partial^2 \psi}{\partial \eta^2} - \alpha^2 \frac{\partial \psi}{\partial t} = -4\pi F(\eta, t) \qquad (3.1)$$

[4] *P.M. Morse and H. Feshbach, Methods of Theoretical Physics (McGraw-Hill, New York, 1953), Chap. 7.*

which obeys appropriate boundary and initial conditions and where ψ is defined in the half-space $\eta \geq 0$. The general solution of Eq. (3.1) may be written

$$\psi(\eta,t) = \int_0^t dt' \int_0^\infty d\eta' \, F(\eta', t') \, G(\eta,t;\eta',t') + \frac{\alpha^2}{4\pi} \int_0^\infty d\eta' \, [\psi G]_{t'=0}$$

$$- \frac{1}{4\pi} \int_0^t dt' \, [G \frac{\partial \psi}{\partial \eta'} - \psi \frac{\partial G}{\partial \eta'}]_{\eta'=0} \qquad (3.2)$$

where G is the appropriate Green's function. For a semi-infinite medium the Green's function can be constructed from those appropriate for an infinite medium. One finds

$$G(\eta,t;\eta',t') = \frac{2}{\alpha} \sqrt{\frac{\pi}{t-t'}} \left\{ \exp \left[\frac{-\alpha^2 (\eta-\eta')^2}{4(t-t')} \right] \pm \exp \left[\frac{-\alpha^2 (\eta+\eta')^2}{4(t-t')} \right] \right\} \qquad (3.3)$$

where the upper sign is to be taken if $\frac{\partial G}{\partial \eta'}$ is to vanish at $\eta' = 0$ (homogeneous Neumann condition) and the lower sign if G is to vanish at $\eta' = 0$ (homogeneous Dirichlet condition). These results will prove useful in obtaining the special-case solutions.

1. Current Density and Magnetic Induction Prior to Melting

Analytic expressions for both the current density and the induction field can be obtained prior to the onset of melting from Eqs. (2.18) and (2.19) and from the boundary conditions in Eqs. (2.22). The last term in Eq. (2.18) is, of course, set equal to zero. Using Eqs. (3.1)-(3.3) and restricting ourselves to times less than t_0, we obtain

$$B(\eta,t) = \frac{\mu j \eta}{2\ell_a} \left(\frac{\mu\sigma}{\pi}\right)^{1/2} \int_0^t \frac{(v_0 t' + 1/2 \, a \, t'^2)}{(t - t')^{3/2}} \exp \left[- \frac{\mu \sigma \eta^2}{4(t-t')} \right] dt' \, . \qquad (3.4)$$

The integral in Eq. (3.4) can be evaluated by making the change of variable

$$r^2 = \frac{\mu \sigma \eta^2}{4(t - t')} \qquad (3.5)$$

and using the easily derived reduction formula

$$\int \frac{e^{-r^2}}{r^{2j}} dr = \frac{-e^{-r^2}}{(2j - 1) r^{2j-1}} - \frac{2}{(2j - 1)} \int \frac{e^{-r^2}}{r^{2j-2}} dr \, . \qquad (3.6)$$

One finds after considerable algebra

$$B(\eta, t) = \frac{\mu j}{\ell_a}(v_0 t + 1/2\, a\, t^2)\ \mathrm{Erfc}\ (r_0)$$

$$+ \frac{2\,\mu^2\sigma j\eta^2}{\ell_a\sqrt{\pi}}\left\{\frac{a\ \mu\sigma\eta^2}{96 r_0^3}\ e^{-r_0^3} - \left[\frac{a\mu\sigma\eta^2}{48} + \frac{v_0 + at}{4}\right]\left[\frac{e^{-r_0^2}}{r_0}\right.\right.$$

$$\left.\left. - \sqrt{\pi}\ \mathrm{Erfc}\ (r_0)\right]\right\} \quad . \tag{3.7}$$

where

$$r_0^2 = \frac{\mu\sigma\eta^2}{4t} \tag{3.8}$$

and where Erfc is the complementary error function

$$\mathrm{Erfc}\ (r_o) = \frac{2}{\sqrt{\pi}} \int_{r_0}^{\infty} e^{-r^2}\, dr \ . \tag{3.9}$$

The current density then follows by direct differentiation in accordance with Eq. (2.19). We find

$$J(\eta,t) = -\frac{\mu\sigma j}{\ell_a\sqrt{\pi}}\left\{(v_0 + at)\left[\left(\frac{4t}{\mu\sigma}\right)^{1/2} e^{-r_0^2} - \sqrt{\pi}\,\eta\ \mathrm{Erfc}\ (r_0)\right]\right.$$

$$\left. - \frac{a\mu\sigma}{4}\left[\left(\frac{4t}{\mu\sigma}\right)^{3/2}\frac{e^{-r_0^2}}{3} - \frac{2\eta^2}{3}\left(\frac{4t}{\mu\sigma}\right)^{1/2} e^{-r_0^2} + \frac{2\sqrt{\pi}\eta^3}{3}\ \mathrm{Erfc}\ (r_0)\right]\right\} \tag{3.10}$$

2. Temperature Profile Prior to Melting for Negligible Ohmic Heating

As indicated previously, ohmic heating is frequently negligible in cases of practical interest. In such a case, Eq. (2.20) can be solved prior to the time of melting via the techniques discussed previously. Equation (2.21) is used to supply the boundary condition on $\frac{\partial T}{\partial \eta}$ at $\eta = 0$ and the "melting term" in both Eqs. (2.20) and (2.21) is set equal to zero. We find for times $t < t_0$

$$T(\eta,t) = T_0 + \frac{Q}{\sqrt{\pi\rho Ck}} \int_0^t \frac{\exp\left[-\frac{\rho C\eta^2}{4k(t-t')}\right]}{(t - t')^{1/2}}\, dt' \ . \tag{3.11}$$

The integral can be evaluated as before by using Eqs. (3.5) and (3.6) and we find

$$T(\eta,t) = T_0 + \frac{Q}{k}\left[\left(\frac{4kt}{\pi\rho C}\right)^{1/2} \exp\left(\frac{-\rho C\eta^2}{4kt}\right) - \eta\ \mathrm{Erfc}\ \left(\frac{\sqrt{\rho C}}{\sqrt{4kt}}\eta\right)\right] \ . \tag{3.12}$$

From Eq. (3.12) an approximate time to melting t_m can be derived by setting $\eta = 0$ and $T(\eta,t) = T_m$. We obtain

$$t_m = \frac{\pi \rho C k (T_m - T_0)^2}{4Q^2} \quad . \tag{3.13}$$

3. Steady-State Melting for Negligible Ohmic Heating

For sufficiently long times, one might expect that Eqs. (2.18)-(2.21) would have a steady-state solution provided the resistive-heating term can be neglected. Assuming such a solution, we obtain from Eqs. (2.18) and (2.20)

$$\frac{d^2B}{d\eta^2} + \mu\sigma v_m \frac{dB}{d\eta} = 0 \tag{3.14}$$

and

$$k \frac{d^2T}{d\eta^2} + \rho C v_m \frac{dT}{d\eta} = 0 \tag{3.15}$$

where

$$v_m = \frac{ds}{dt} \tag{3.16}$$

is the (constant) propagation velocity of the melting surface.

Equations (3.14) and (3.15) have the obvious solutions

$$B = \mu j e^{-\mu\sigma v_m \eta} \tag{3.17}$$

$$T = (T_m - T_0) e^{-\rho C v_m \eta/k} + T_0 \quad . \tag{3.18}$$

Furthermore, from (2.21) and (3.18) we obtain for the steady-state melting velocity

$$v_m = \frac{Q}{\rho C (T_m - T_0) + L\rho} \quad . \tag{3.19}$$

The nontrivial solution arises when Q, the constant flux radiated from the arc, is nonzero. Therefore, one can expect such a steady solution to be achieved provided that the arc is in contact with x_0 long enough for a steady state to be achieved.

B. Numerical Analysis

To solve Eqs. (2.18)-(2.21), we divided the (η,t) plane into a grid, represented the derivatives by second-order finite differences, and solved by the standard implicit technique.[5] Not only were numerical calculations carried out for cases of general interest, but also for cases corresponding to the special-case analytic solutions in Sec. III A. We could thereby check the validity of the computer program as well as determine suitable step sizes $\Delta\eta$ and Δt. For all cases undertaken, we found acceptable values of $\Delta\eta$ and Δt of the order of 5×10^{-6} m and 5×10^{-8} s, respectively, while the arc was in contact with the point x_0; some time after the arc had passed, however, and radiation was assumed negligible, we were able to increase Δt by an order of magnitude or more.

We have performed calculations in which we both neglected and included the resistive-heating losses. We consistently found, however, that for all cases of interest to us (very high-temperature arcs and rails whose thickness was greater than or comparable to a skin depth), the resistive contributions were utterly negligible. Therefore, in the discussion which follows, the resistive terms have been neglected. Doing so immensely facilitates numerical calculations because the speed at which the magnetic field diffuses into the rail is much larger than the speed at which the temperature diffuses. Consequently, when considering the negligible resistive losses, it was necessary to employ far more grid points in the calculation than was necessary in the simpler case.

C. Analysis of Jamison-Burden Experimental Results

In a recent experiment, Jamison and Burden (JB) have employed a rail gun[6] made of copper rails with the projectile driven by a copper-vapor arc to accelerate a 2.5g projectile to about a kilometer per second. Values of the current, breech voltage, velocity, acceleration, and arc length were measured at several points along the gun tube. These data were then used as input parameters in the numerical solution of Eqs. (2.20) and (2.21). [The resistive contribution to the temperature rise was found to be negligible in this experiment. Therefore, J was set equal to zero in Eq. (2.20) and Eqs. (2.18) and (2.19) were not solved.] In doing such an analysis of course it is necessary to assume that all significant parameters associated with the rail gun change in a quasi-static manner since the original derivations were for steady-state operation.

In Table I are shown the material properties of copper used in the calculation as well as the experimental data taken at two points along the gun tube, at $x_0 = 0.156$m and $x_0 = 0.51$m. The first five entries in the columns headed

---

[5] *B. Carnahan, H.A. Luther, and J.O. Wilkes, Applied Numerical Methods (Wiley, New York, 1969), Chap. 7.*

[6] *K.A. Jamison and H.S. Burden, "A Laboratory Arc-Driven Rail Gun," Ballistic Research Laboratory Report No. ARBRL-TR-02502, June 1983 (AD A131153).*

TABLE I. Experimental Data and Input Parameters for Numerical Calculations

Material Properties of Rails

Quantity	Value
k	400 watts /(m K)
σ	5.8×10^7 mho/m
L	2.1×10^5 J/kg
C	390 J/(K kg)
ρ	8.9×10^3 kg/m^3
T_m	1360 K

Data

Quantity	Values at $x_0 = 0.156$m	Values at $x_0 = 0.51$m
v_0	560 m/s	757 m/s
a	5.8×10^5 m/s^2	1.69×10^5 m/s^2
j	3.94×10^6 A/m	1.97×10^6 A/m
V_0	156 volts	132 volts
ℓ_a	3.3 cm	6.8 cm
t_0	58 μs	90 μs
T_b	1.69×10^4 K	1.14×10^4 K

"DATA" were taken directly from the experimental results[7] and are self-explanatory. It should be mentioned, however, that the muzzle voltage V_0 was not directly measured in the experiment. The breech voltage was measured, however, and the muzzle voltage estimated by measuring and subtracting the inductive contribution to the breech voltage. The last two entries in the table, needed in the numerical calculations, were calculated for each point in terms of the experimental data. The parameter t_0 was calculated by using Eq. (2.4), with the actual initial velocity v_0 substituted for the quantity $\sqrt{2ax_0}$, and the boundary temperature T_b from the approximate expression derived in the Appendix:

$$T_b = \left(\frac{jV_0}{4\sigma_s \ell_a}\right)^{1/4} . \qquad (3.20)$$

[7] *K.A. Jamison and H.S. Burden (private communication).*

Results of the numerical calculation at the point $x_0 = 0.156$m are shown in Figs. 2-5. In Fig. 2 are four temperature profiles. Profile A shows the temperature distribution as a function of depth just prior to the time melting begins. The temperature at $\eta = 0$ is about 1335 K and the arc has been in contact with x_0 for 12 μs. A nonnegligible rise in the rail temperature can be seen for about 100 μm beyond the rail surface at $\eta = 0$. Profile B shows the temperature distribution within the rail at time $t = 57$ μs. As can be seen from the value of t_0 in Table I, this time is just prior to the time that the arc leaves x_0. The temperature at $\eta = 0$ is, of course, $T_m = 1360$ K. The extent to which Profile B is approximated by the steady-state result can be seen by comparing Profiles B and C, since Profile C is just a graph of Eq. (3.18). As can be seen, the steady-state result has nearly been reached. Finally, Profile D shows the temperature distribution at $t = 90$ μs, i.e., long after the arc has passed. Melting has ceased as would be expected and the temperature at the surface has fallen by nearly a factor of two. It should be noted that in terms of the original location of the rail surface, curves B and D have been shifted by about 60 μm (see Fig. 5) because of rail melting.

In Fig. 3 is plotted the temperature of the rail surface (located at $\eta = 0$) as a function of time. We observe a steady, rapid rise in the temperature for about the first fourteen microseconds until the melting temperature T_m is reached. The time to melting can be predicted analytically from Eq. (3.13). Subsequently, the temperature at the surface remains constant until the arc has passed ($t \sim 59$ μs). Continuous cooling then follows as heat is conducted into the bulk of the rail.

In Fig. 4 is shown the velocity of recession of the melting surface, v_m, as a function of time. We see a rapid rise in the velocity during the early stages of melting followed by a slower approach to the steady value of 1.7 m/s, predicted by Eq. (3.19). Just prior to the time the arc has left x_0 and melting has ceased, the surface velocity has approached about 85% of the steady-state value.

Finally, in Fig. 5, we show the position of the rail surface relative to its initial position (the parameter s defined in Sec. I) as a function of time. As can be seen, between fifty and sixty microns of the rails will have melted during the time in which the arc was in contact with x_0. After the arc has passed no further melting occurs.

At the point $x_0 = 0.51$m, to which the second set of data in Table I applies, we have from Eq. (2.4), $t_0 = 90$ μs. From Eq. (3.13), however, the time to melting t_m is 332 μs so we conclude that no melting of the rails occurs at this point.

D. Other Calculations

The JB experiment is the only case of which we have sufficient experimental data to allow us to calculate rail-melting phenomena using only measured quantities. To get some idea of what the effects might be in other guns, however, we have used results calculated in our previous work as input for our

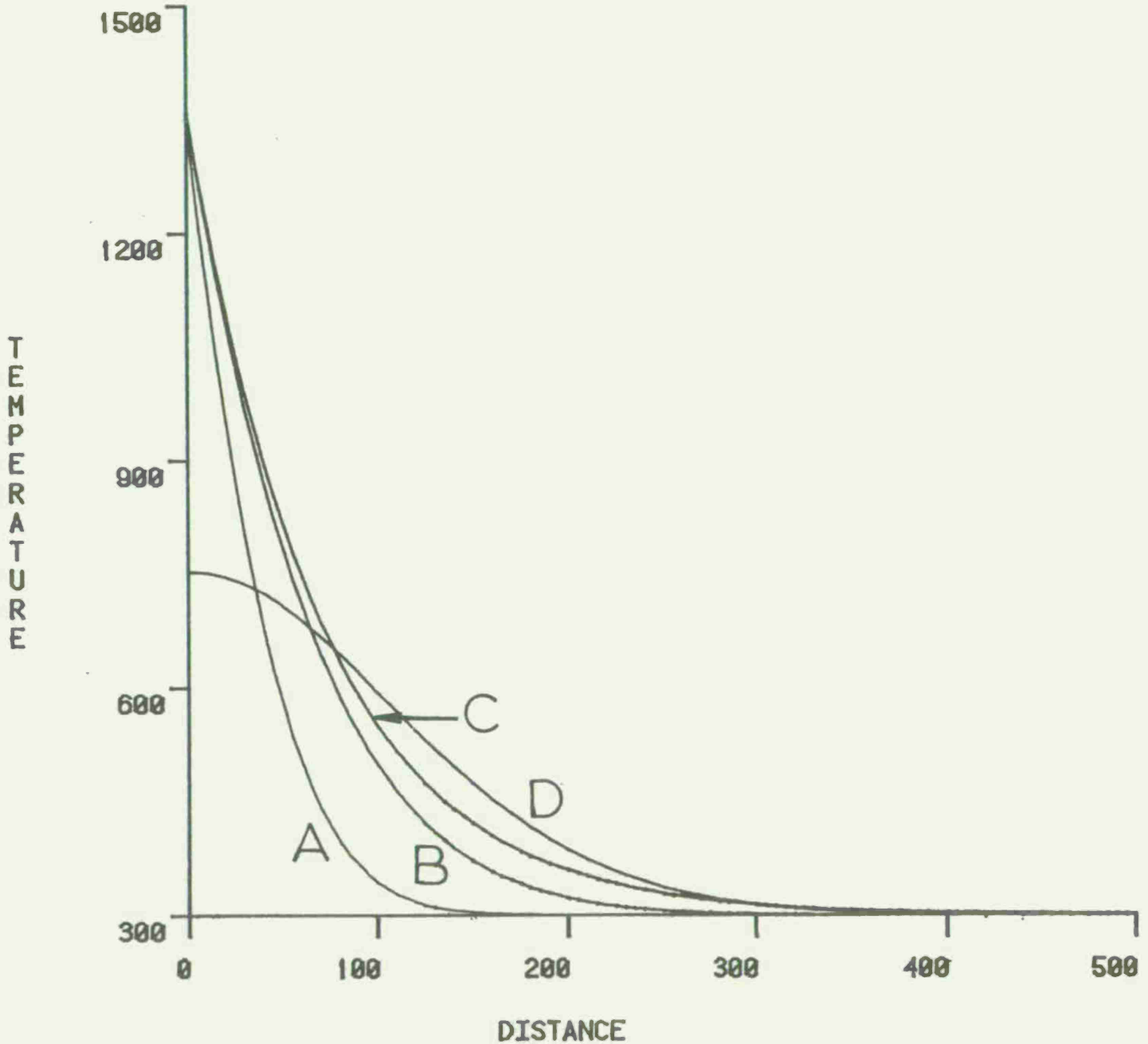

Figure 2. Temperature profiles as a function of distance behind the melting surface (η); A, at t = 12 μs (just prior to melting); B, at t = 57 μs (just prior to the cessation of melting); C, steady-state melting profile; D at t = 90 μs (long after the arc has passed). The distance scale is in microns.

Figure 3. Surface temperature vs. time. The time scale is in microseconds.

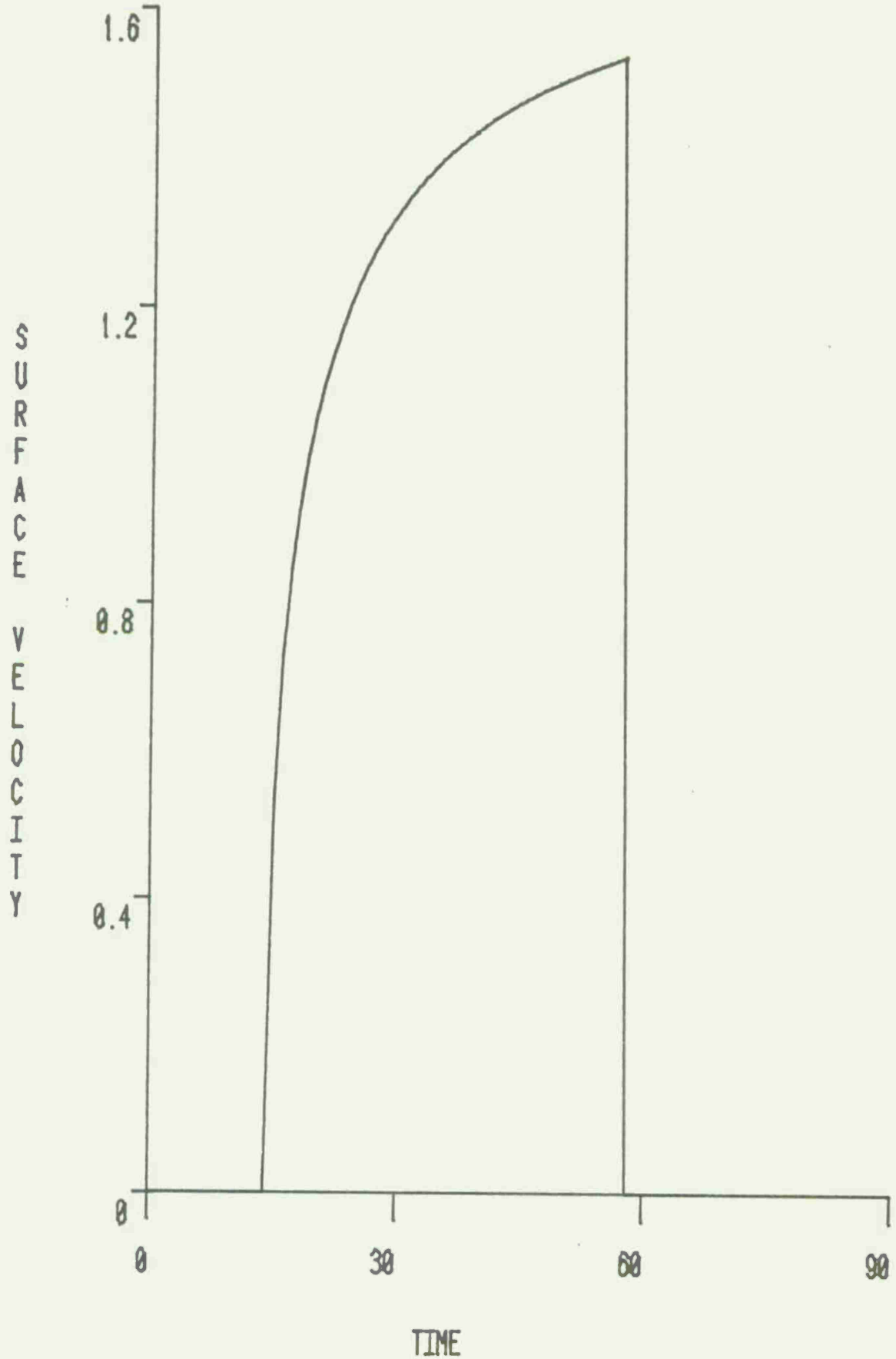

Figure 4. Velocity of melting surface, v_m, in m/s, vs. time, in μs.

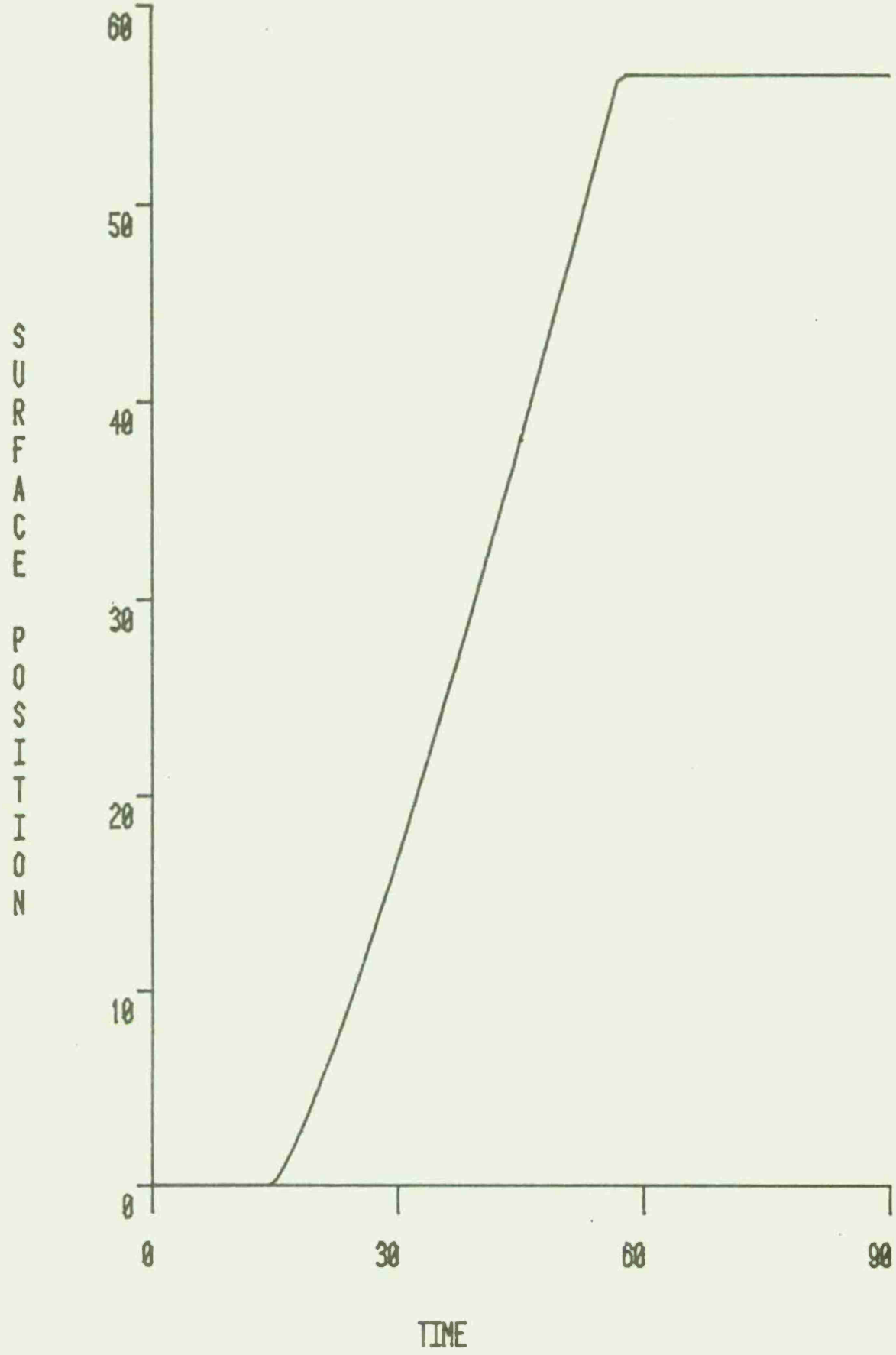

Figure 5. Position of solid surface relative to initial position, s, in microns, vs. time, in microseconds.

thermal-energy transport model. Surely the greatest source of uncertainty in these data is for the arc length ℓ_a. Indeed, this quantity was unknown in our previous work and a value of the order of 10 cm was assumed, as had been done in previous arc-dynamic calculations.[8]

Input data and results for two calculations are shown in Table II. The first is for a gun comparable in size to that used by Rashleigh and Marshall (RM) in their well-known experiment,[9] and the second was for a larger gun comparable to that recently constructed by Deis, McNab, and coworkers.[10] Two-dimensional calculations[2] to determine properties of the arc in both these guns were undertaken in our previous work.

TABLE II. Results for RM and Large Guns

Quantity	RM	Large Gun
a	$1.5 \times 10^7 m/s^2$	$1.13 \times 10^6 m/s^2$
ℓ_a	9.8 cm	9.9 cm
V_0	50 volts	171 volts
j	$1.92 \times 10^7 A/m$	$1.47 \times 10^7 A/m$
T_b	1.44×10^4 K	1.83×10^4 K
t_m	51 μs	7.6 μs
v_m	0.88 m/s	2.3 m/s
t_0(at $x_0 = 0$)	114 μs	419 μs
t_0 (at $x_0 = 0.5$ m)	25 μs	89 μs
t_0 (at $x_0 = 2$ m)	13 μs	47 μs
t_0 (at $x_0 = 4$ m)	9 μs	33 μs
t_0 (at $x_0 = 5$ m)	8 μs	29 μs

The first few entries in the table were taken directly from Ref. 2. The quantities T_b, t_m, v_m, and t_0 were than calculated from Eqs. (3.20), (3.13), (3.19) and (2.4), respectively. Several numerical calculations were undertaken

[8] *I.R. McNab, "Electromagnetic Acceleration by a High Pressure Plasma," J. Appl. Phys. 51, 2549 (1980).*

[9] *S.C. Rashleigh and R.A. Marshall, "Electromagnetic Acceleration of Macroparticles to High Velocities," J. Appl. Phys. 49, 2540 (1978).*

[10] *"Laboratory Demonstration Electromagnetic Launcher-EMACK," Commissioning Test Results, Westinghouse R&D Center, Pittsburgh, PA.*

to make certain that resistive heating was negligible and that Eq. (3.13) adequately predicted the time to melting.

Graphical results will not be presented since they are similar qualitatively to those shown in Figs. 2-5. It is interesting, however, to note that for the RM case, results similar to those for the JB experiment are observed, as can be seen from Table II. Specifically, the calculations predict rail melting toward the breech end of the gun ($x_0 = 0$), but none farther down the gun tube, say, at $x_0 = 0.5$m. For the larger rail gun, the calculated results suggest melting throughout an entire 5m gun tube, though the greatest amount by far is toward the breech end of the gun.

IV. SUMMARY AND DISCUSSION

We have developed a model, which when used in conjunction with calculated or experimentally measured properties of the arc, can predict thermal damage on the surfaces of the rails. Calculations have been undertaken using as input data the experimental results of Jamison and Burden, as well as for input data obtained theoretically in previous work. Results indicate substantial melting very close to the breech of the gun, with little or none farther out on the gun tube.

A number of approximations are made in order to make the calculations feasible (see Sec. I) but in every case the approximations, if anything, overestimate the amount of wear on the rail surface. When using the measured data as input, the major source of error probably lies in the determination of the boundary temperature of the arc T_b. To determine this temperature one must rely on the experimentally measured muzzle voltage V_0. It has been pointed out previously,[8] however, that this measured voltage probably includes a substantial contribution from the contact potential at the rail-arc interfaces. Consequently, the potential drop across the arc, which should actually be used in Eq. (3.20), is likely to be smaller than the measured value. For instance, if we assumed that only one-third of the measured muzzle voltage corresponds to the potential across the arc, as McNab[8] has done, the model predicts for the JB data no melting even at the point $x_0 = 0.156$m. Again, the use of too large a potential in the model calculations will predict too large a boundary temperature and, thus, greater erosion than in fact occurs. The greatest source of error in using theoretically obtained input data is clearly in our ignorance of accurate values of the arc length ℓ_a.

Uncertainty in these input data suggests the need for additional work, both theoretical and experimental. On the theoretical side, two major problems are evident. First, it would be very desirable to obtain a theoretical prediction of the arc length in rail-gun accelerators. A study of this problem is difficult and would be likely to involve a rather detailed understanding of how arcs are formed initially and how they change during the course of acceleration. A second theoretical problem is to investigate the nature of the contact potential that no doubt exists at the rail-arc interface. A theoretical estimate of the magnitude of this potential would clearly allow us to

ascertain what fraction of the measured potential actually results from a resistive drop across the plasma.

From the experimental viewpoint, more data concerning the properties of the arc at various points along the gun tube are much needed. Jamison and Burden have made significant progress in the problem of arc diagnostics, as is evident from the data quoted herein, but more work remains to be done. Some experimental analysis of rail erosion would also be beneficial. Work on this problem has been initiated by Jamison and Burden using the experimental nuclear technique of thin-layer activation.[11] Some preliminary results have been obtained but more detailed measurements are desirable.

It is hoped that as more data concerning arc properties become available, the model under study here can be used more successfully to predict thermal damage to the rails. It would also be beneficial in the future to study other types of damage (say, mechanical) both theoretically and experimentally.

[11] *See, e.g., A. Niiler and S.E. Caldwell, "The $^{56}Fe(p,n)^{56}Co$ Reaction in Steel Wear Measurement," Nucl. Inst. and Methods 138, 179 (1976).*

ACKNOWLEDGEMENT

I am grateful to J.H. Batteh for several helpful discussions, and to K.A. Jamison and H.S. Burden for providing me with the data used in the calculations.

REFERENCES

1. J.D. Powell and J.H. Batteh, "Plasma Dynamics of an Arc-Driven, Electromagnetic, Projectile Accelerator," J. Appl. Phys. 52, 2717 (1981). See also "Plasma Dynamics of an Arc-Driven Rail Gun," Ballistic Research Laboratory Report No. ARBRL-TR-02267, September 1980 (AD A092345).

2. J.D. Powell and J.H. Batteh, "Two-Dimensional Plasma Model for the Arc-Driven Rail Gun," J. Appl. Phys. 54, 2242 (1983). See also J.D. Powell, "Two-Dimensional Model for Arc Dynamics in the Rail Gun," Ballistic Research Laboratory Report No. ARBRL-TR-02423, October 1982 (AD A120046).

3. H.G. Landau, "Heat Conduction in a Melting Solid," Quart. Appl. Math. 8, 81 (1950).

4. P.M. Morse and H. Feshbach, Methods of Theoretical Physics (McGraw-Hill, New York, 1953), Chap. 7.

5. B. Carnahan, H.A. Luther, and J.O. Wilkes, Applied Numerical Methods (Wiley, New York, 1969), Chap. 7.

6. K.A. Jamison and H.S. Burden, "A Laboratory Arc-Driven Rail Gun," Ballistic Research Laboratory Report No. ARBRL-TR-02502, June 1983 (AD A131153).

7. K.A. Jamison and H.S. Burden (private communication).

8. I.R. McNab, "Electromagnetic Acceleration by a High Pressure Plasma," J. Appl. Phys. 51, 2549 (1980).

9. S.C. Rashleigh and R.A. Marshall, "Electromagnetic Acceleration of Macroparticles to High Velocities," J. Appl. Phys. 49, 2540 (1978).

10. "Laboratory Demonstration Electromagnetic Launcher-EMACK," Commissioning Test Results, Westinghouse R&D Center, Pittsburgh, PA.

11. See, e.g., A. Niiler and S.E. Caldwell, "The ^{56}FE(p,n)^{56}Co Reaction in Steel Wear Measurement," Nucl. Inst. and Methods 138, 179 (1976).

APPENDIX A

APPENDIX A

In this appendix we will be concerned with deriving an approximate expression for the boundary temperature of the arc in terms of easily measured experimental parameters. For purposes of calculation, we will neglect the position dependence of the arc conductivity and radiation mean free path and will assume the condition $w << \ell_a$. As has been discussed before, neglecting the position dependence in these two quantities does not significantly affect the results, whereas the second condition is generally met in experiments of interest.

Under these assumptions the equation obeyed by the arc temperature is[2]

$$\frac{d^2 T^4}{dy^2} = - \frac{3j^2}{4\sigma_s \sigma\lambda \ell_a^2} \tag{A.1}$$

where σ corresponds to the arc conductivity and λ to its mean free path. Integrating and employing the obvious symmetry condition. (See Fig. 1.)

$$\left(\frac{dT}{dy}\right)_{y = -w/2} = 0 \quad , \tag{A.2}$$

we find

$$\frac{dT^4}{dy} = \frac{-3j^2 w}{8\sigma_s \sigma \lambda \ell_a^2} (1 + 2y/w) \quad . \tag{A.3}$$

A second integration yields

$$T^4 = \frac{-3j^2 w^2}{8\sigma_s \sigma \lambda \ell_a^2} (y/w + y^2/w^2) + C_1 \tag{A.4}$$

where C_1 is a constant.

Now, by assumption, the flux at $y = 0$ satisfies the condition

$$q\ (y = 0) = 2\sigma_s T_b^4 \quad . \tag{A.5}$$

However, if energy transport within the arc occurs by radiation heat conduction, then

$$q = - \frac{4\sigma_s \lambda}{3} \frac{dT^4}{dy} \quad . \tag{A.6}$$

Simultaneous use of (A.4) - (A.6) then yields for the boundary temperature

$$T_b = \left(\frac{w_j^2}{4\sigma_s \sigma \ell_a^2}\right)^{1/4} . \qquad (A.7)$$

However, the potential drop across the plasma or the "muzzle voltage" can be written[2]

$$V_0 = \frac{jw}{\sigma \ell_a} , \qquad (A.8)$$

so in terms of experimentally measured parameters

$$T_b = \left(\frac{jV_0}{4\sigma_s \ell_a}\right)^{1/4} . \qquad (A.9)$$

DISTRIBUTION LIST

No. of Copies	Organization
12	Administrator Defense Technical Info Center ATTN: DTIC-DDA Cameron Station Alexandria, VA 22314
1	Office Under Secretary of Defense Research & Engineering ATTN: Mr. Ray Thorkildsen Room 3D1089, The Pentagon Washington, DC 20301
1	Deputy Under Secretary of Defense Research & Engineering Room 3E114, The Pentagon Washington, DC 20301
3	Director Defense Advanced Research Projects Agency ATTN: Dr. Joseph Mangano Dr. Gordon P. Sigman Dr. Harry Fair 1400 Wilson Boulevard Arlington, VA 22209
1	Office of Assistant Secretary of the Army ATTN: RDA, Dr. Joseph Yang Room 2E672, The Pentagon Washington, DC 20310
1	HQDA (DAMA-ARZ-A/Dr. Richard Lewis) Washington, DC 20310
1	Commander US Army Materiel Development & Readiness Command ATTN: DRCDMD-ST 5001 Eisenhower Avenue Alexandria, VA 22333
1	Commander US Army Materiel Development & Readiness Command ATTN: DRCLDC, Mr. Langworthy 5001 Eisenhower Avenue Alexandria, VA 22333
1	Commander US Army Armament, Munitions & Chemical Command Armament Research & Development Center ATTN: DRSMC-TDC (D) Dover, NJ 07801
6	Commander US Army Armament, Munitions & Chemical Command Armament Research & Development Center ATTN: DRSMC-TSS (D) DRSMC-LCA, Mr. J.A. Bennett, Dr. T. Gora, Dr. P. Kemmy DRSMC-SCA, Mr. W.R. Goldstein Dover, NJ 07801
1	Commander US Army Armament, Munitions & Chemical Command ATTN: DRSMC-LEP-L (R) Rock Island, IL 61299
1	Commander Armament Research & Development Center (Benet Laboratory) US Army Armament, Munitions & Chemical Command ATTN: DRSMC-LCB-TL Watervliet, NY 12189
1	Commander US Army Aviation Research & Development Command ATTN: DRDAV-E 4300 Goodfellow Boulevard St. Louis, MO 63120
1	Director US Army Air Mobility Research & Development Laboratory Ames Research Center Moffett Field, CA 94035
1	Commander US Army Communications Research & Development Command ATTN: DRSEL-ATDD Fort Monmouth, NJ 07703

DISTRIBUTION LIST

No. of Copies	Organization
1	Commander US Army Electronics R&D Command Technical Support Activity ATTN: DELSD-L Fort Monmouth, NJ 07703
1	Commander US Army Missile Command ATTN: DRSMI-R Redstone Arsenal, AL 35898
1	Commander US Army Missile Command ATTN: DRSMI-YDL Redstone Arsenal, AL 35898
1	Commander US Army Tank Automotive Command ATTN: DRSTA-TSL Warren, MI 48090
1	Director US Army TRADOC Systems Analysis Activity ATTN: ATAA-SL White Sands Missile Range NM 88002
2	Commandant US Army Infantry School ATTN: ATSH-CD-CSO-OR Fort Benning, GA 31905
2	Commander US Army Research Office ATTN: Dr. Fred Schmiedeshoff Dr. M. Ciftan P.O. Box 12211 Research Triangle Park, NC 27709
1	Commander Naval Air Systems Command ATTN: John A. Reif, AIR 350B Washington, DC 20360
4	Commander Naval Surface Weapons Center ATTN: Mr. H. B. Odom, Code F-12 Dr. M. F. Rose, Code F-04 Mr. P. T. Adams, Code G-35 Mr. D. L. Brunson, Code G-35 Dahlgren, VA 22448
2	Commander US Naval Research Laboratory ATTN: Dick Ford, Code 4774 Washington, DC 20375
1	HQ AFSC/XRB/SDOA CPT Dennis Kirlin Andrews AFB, MD 20334
2	AFATL/DLDB (Lanny Burdge, Bill Lucas) Eglin AFB, FL 32542
1	AFATL (Richard Walley) Eglin AFB, FL 32542
1	AFWL (Dr. William L. Baker) Kirtland AFB, NM 87117
1	AFWL/NTYP (John Generosa) Kirtland AFB, NM 87117
1	AFWL/SUL Kirtland AFB, NM 87117
1	AFAPL (Dr. Charles E. Oberly) Wright-Patterson AFB, OH 45433
1	AFWAL/POOS-2 (CPT Jerry Clark) Wright-Patterson AFB, OH 45433
1	Director Brookhaven National Laboratory ATTN: Dr. James R. Powell, Bldg. 129 25 Brookhaven Avenue Upton, NY 11973
1	Director Lawrence Livermore National Laboratory ATTN: Dr. R. S. Hawke, L-156 P.O. Box 808 Livermore, CA 94550
2	Director Los Alamos National Laboratory ATTN: Dr. Clarence M. Fowler, MS970 Dr. Denis R. Peterson, MS985 P.O. Box 1663 Los Alamos, NM 87545

DISTRIBUTION LIST

No. of Copies	Organization
3	NASA-LeRC-MS 501-7 ATTN: Bill Kerslake Frank Terdan Mike Brasher 2100 Brookpark Rd. Cleveland, OH 44135
1	Boeing Aerospace Company ATTN: J.E. Shrader P.O. Box 3999 Seattle, WA 94124
1	General Dynamics ATTN: Dr. Jaime Cuadros P.O. Box 2507 Pamona, CA 91766
3	GT Devices ATTN: Dr. Derik Tidman Dr. Shyke Goldstein Dr. Neils Winsor 5705-A General Washington Drive Alexandria, VA 22312
1	Physics International ATTN: Dr. A.L. Brooks 2700 Merced Street San Leandro, CA 94577
2	R&D Associates ATTN: Mr. Ronald Cunningham Dr. Peter Turchi P.O. Box 9695 Marina del Rey, CA 90291
1	Science Applications, Inc. ATTN: Dr. Jad H. Batteh 1503 Johnson Ferry RD, Suite 100 Marietta, GA 30062
1	Science Applications, Inc. Corporate Headquarters ATTN: Dr. Frank Chilton 1200 Prospect Street La Jolla, CA 92038
1	Unidynamics/Phoenix, Inc. ATTN: W.R. Richardson P.O. Box 2990 Phoenix, AZ 85062
2	Vought Corporation ATTN: William B. Freeman Charles Haight P.O. Box 225907 Dallas, TX 75265
2	Westinghouse Research & Development Laboratory ATTN: Dr. Ian R. McNab Dr. Y. Thio 1310 Beulah RD Pittsburgh, PA 15253
2	Massachusetts Institute of Technology Francis Bitter National Magnet Lab ATTN: Dr. Henry H. Kolm, Dr. Peter Mongeau NW-14-3102 170 Albany Street Cambridge, MA 02139
1	University of Texas Center of Electromechanics ATTN: Mr. William F. Weldon 167 Taylor Hall Austin, TX 78712

Aberdeen Proving Ground

Dir, USAMSAA
ATTN: DRXSY-D
DRXSY-MP, H. Cohen
Cdr, USATECOM
ATTN: DRSTE-TO-F
Cdr, USACRDC
ATTN: DRSMC-CLB-PA
DRSMC-CLN
DRSMC-CLJ-L

USER EVALUATION OF REPORT

Please take a few minutes to answer the questions below; tear out this sheet, fold as indicated, staple or tape closed, and place in the mail. Your comments will provide us with information for improving future reports.

1. BRL Report Number _____

2. Does this report satisfy a need? (Comment on purpose, related project, or other area of interest for which report will be used.)

_____

_____

_____

3. How, specifically, is the report being used? (Information source, design data or procedure, management procedure, source of ideas, etc.) _____

_____

_____

4. Has the information in this report led to any quantitative savings as far as man-hours/contract dollars saved, operating costs avoided, efficiencies achieved, etc.? If so, please elaborate.

_____

_____

5. General Comments (Indicate what you think should be changed to make this report and future reports of this type more responsive to your needs, more usable, improve readability, etc.) _____

_____

_____

_____

6. If you would like to be contacted by the personnel who prepared this report to raise specific questions or discuss the topic, please fill in the following information.

Name: _____

Telephone Number: _____

Organization Address: _____

_____

_____